Intelligent Traffic Signal System for Isolated Intersections

Dynamic Pedestrian Accommodation

George X. Lu, Yi Zhang, and David A. Noyce

One critical issue of traffic control is the optimization of signalized intersections for improved multimodal safety and operations. Accommodating pedestrian traffic at intersections is challenging because the demands of multimodal service compete fiercely on limited green time resources. The *Highway Capacity Manual* prescribes that the parallel vehicle green must exceed "Walk" plus pedestrian clearance interval (PCI) timed by a design walking speed. This static PCI timing is unsafe because seniors and children are likely to be slower than the design pedestrian. Furthermore, a vehicle-flow issue arises when the prolonged PCI exceeds the operationally efficient parallel green: additional vehicle right-of-way, unnecessary for operational efficiency, preempts green time from conflicting phase(s) and increases intersectionwide queuing delays. Queuing delays necessitate a trade-off between competing multifaceted traveler needs. Fuzzy logic control (FLC) proves effective, flexible, and robust in handling competing objectives. With the dynamic PCI concept, this research developed an intelligent traffic signal system that performed friendly pedestrian accommodation and also incorporated FLC into fulfilling multifaceted vehicle needs. The potential benefits from the new system optimized with a genetic algorithm were quantified through a comparison with a standard dual-ring, eight-phase, vehicle-actuated controller, conventionally cited as NEMA (National Electrical Manufacturers Association) control. Microsimulation experiments revealed that the current countermeasure, which lowered PCI timing design speed to strengthen crossing safety, was operationally deficient. The existing timing standard cannot offer adequate safety for all pedestrians, and the NEMA system omits multifaceted vehicle needs in control logic. In contrast, the FLC system fully protects all pedestrians through dynamic PCI and smartly serves manifold vehicle needs well. The FLC system outperforms the NEMA control by embodying a reasonable trade-off between competing objectives in the management of an isolated intersection.

The contemporary transportation research community faces increasing challenges in providing the traveling public with safer, efficient, and reliable multimodal transportation infrastructure systems. Today's transportation problems have become increasingly complex in nature because their scopes have been rapidly expanding far beyond the traditional realm. "A large number of variables are involved; the parametric relationships among them are not well-understood; a large volume of incomplete data is involved, and the goals and constraints are many and the priorities among the stakeholders are unclear" (*1,* p. 455). Philosophically, "as the complexity of a system increases, our ability to make precise and yet significant statements about its behaviors diminishes, and significance and complexity become almost mutually exclusive characteristics," which implies that a multitude of transportation problems are profoundly difficult to resolve in traditional approaches (*2,* p. 363). Artificial intelligence methodologies are proved instrumental to modeling the behaviors of complex phenomena while giving researchers the latitude to "acknowledge some level of ignorance," which "provides the opportunity to examine the problem from different perspectives and compare the results" (*1,* p. 455). There has been vastly growing interest in applying artificial intelligence and relevant advanced computing techniques to address the complex issues essentially associated with safety, operations, and other dimensions of multimodal transportation infrastructure systems (*3*).

Perhaps one of the most critical issues that challenge traffic engineers is to comprehensively optimize the performance of urban signalized intersections where motorized and nonmotorized travelers are busily transported in dynamic operations. The signalization improvement has been recognized as one of the most cost-effective ways of mitigating roadway congestion and ameliorating multimodal transportation safety (*4*). In traffic engineering, intersection control pursues dual principal objectives: "(*a*) ensure safety for all intersection users; (*b*) promote efficient movement of all users through the intersection" (*5*). Alternatively, the dominant considerations in the operation of an isolated intersection are safe and efficient traffic movement, limiting vehicle delay, and increasing intersection capacity (*6*). To achieve those goals is a difficult task because generally safety and efficiency are mutually competing (or even conflicting), rather than reinforcing or complementary, issues (*5*). Fuzzy logic control (FLC) has been proved more effective, flexible, and robust than traditional controls in tackling complex systems in which conflicting objectives, subjective perception, imprecise data, and vague decision-making criteria play critical roles (*1, 7*). Therefore, the variability and complexity in intersection signalization can be effectively modeled in an FLC-based approach for manifold improvement purposes.

U.S. safety data reveal that a pedestrian is killed or injured in a traffic accident every 120 or 8 min, respectively (*8*). Intersection crosswalks are particularly hazardous to seniors and children. In 2008, 35% of pedestrian fatalities among people 60 and older occurred at intersections, compared with 20% for those younger

G. X. Lu, Transportation Research Center, University of Vermont, Farrell Hall 118, 210 Colchester Avenue, Burlington, VT 05405. Y. Zhang, Transportation Engineering Division, 1241 Engineering Hall, and D. A. Noyce, Traffic Operations and Safety Laboratory, 1204 Engineering Hall, Department of Civil and Environmental Engineering, University of Wisconsin–Madison, 1415 Engineering Drive, Madison, WI 53706-1691. Corresponding author: G. X. Lu, xlu@uvm.edu.

Transportation Research Record: Journal of the Transportation Research Board, No. 2259, Transportation Research Board of the National Academies, Washington, D.C., 2011, pp. 96–111.
DOI: 10.3141/2259-09

than 60 (*9*). Alarmed by the tragic casualties, cities nationwide are increasingly seeking novel control strategies to make pedestrian crosswalks safer (*10*). Although many research endeavors have led to improved movement efficiency for motorized traffic at signalized intersections, the effect of walking speed variability on multimodal safety and operations, along with relevant problems and solutions, remains inadequately researched.

PROBLEM STATEMENT

At a signalized intersection, nonmotorized travelers (mostly pedestrians) are accommodated by a preset phasing and timing scheme. During a pedestrian signal phase, the "Walk" interval displays to release the pedestrians in waiting areas, then the flashing "Don't Walk" interval, which functions as the pedestrian clearance interval (PCI), lasts for a predetermined duration. Finally, the steady "Don't Walk" interval follows to prohibit crossing movements. The *Highway Capacity Manual* (HCM) prescribes the minimum crossing time requirement as follows (*11*):

$$G_p = 3.2 + \frac{L}{S_p} + 2.7\left(\frac{N_{\text{ped}}}{W_E}\right) \quad \text{for} \quad W_E > 10 \text{ ft} \tag{1}$$

$$G_p = 3.2 + \frac{L}{S_p} + 0.27N_{\text{ped}} \quad \text{for} \quad W_E \leq 10 \text{ ft} \tag{2}$$

where

G_p = minimum pedestrian crossing time (s),
L = crosswalk length (ft),
S_p = average pedestrian walking speed (design speed) (ft/s),
N_{ped} = number of pedestrians crossing in a single crosswalk (pedestrians per phase), and
W_E = crosswalk width (ft).

Equations 1 and 2 allocate 3.2 s as the minimal reaction and start-up time to the Walk interval, and the last terms in the equations allocate additional start-up time by using pedestrian volumes. Once the Walk ends, pedestrians just starting to cross an intersection require the PCI for safe clearance. The HCM regulates that the parallel vehicle green interval must equal or exceed the Walk plus the PCI (*11*). The length of PCI, L/S_p, is calculated by a constant design walking speed (S_p), which is critical in determining how much clearance time is actually given to crossing pedestrians. Historical pedestrian studies suggested disparate design standards because the walking speed was found to fluctuate between 1.0 and 8.0 ft/s for different populations (*12–14*). Obviously, it is perilous to provide a uniform PCI length for a cane user and a young runner. Yet this is how an existing traffic signal system operates at an intersection: the *Manual on Uniform Traffic Control Devices* designates 3.5 ft/s as S_p for PCI timing (*15*). The question of what is the most appropriate S_p has kindled a nationwide debate; a countermeasure has been practiced in regard to shortening S_p to lengthen the PCI duration. Section 4E.06 of the manual states, "Where . . . pedestrians who use wheelchairs, routinely use the crosswalk, a walking speed of less than 3.5 fps [ft/s] should be considered in determining the pedestrian clearance time," but no specific value is stipulated (*15*). It is plausible that this countermeasure can be effective to offer adequate crossing safety.

However, an operational problem arises along with the foregoing countermeasure. As Figure 1 shows, when the lengthened PCI_c^{ped} exceeds the parallel green (G_E^{veh}), which is factually required for efficient vehicle movements, the additional green time (G_A^{veh}) resultant from this prolongation is operationally surplus. The longer vehicle right-of-way given by G_A^{veh} has to preempt an additional amount of green time from the next phase (Φ_n^{veh}) and consequently induce more red time (R), which will inflict the whole intersection with increased queuing vehicle delays. Therefore, providing a long but static PCI for variable walking needs will pose a tangible detriment to traffic flow efficiency, rendering the intersection operations systematically suboptimal. This problem deteriorates enormously if a tiny S_p is introduced: once those expeditious pedestrians have vacated the

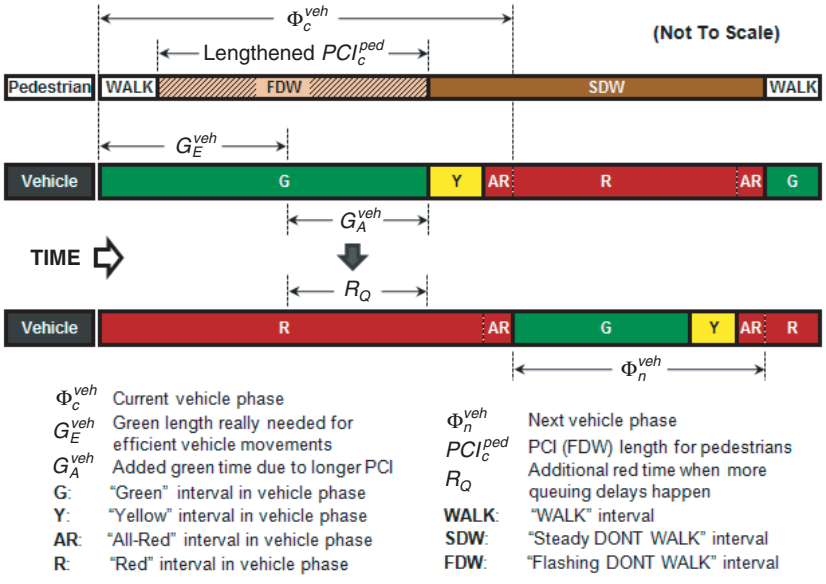

FIGURE 1 Illustration of pedestrian crossing safety versus traffic movement efficiency problem.

crosswalks, the residual PCI time is purely idle and G_A^{veh} is underused; simultaneously, the queuing vehicles stopped by R_Q are keen to receive their right-of-way. Hence, it is essential to procure a sensible compromise between these competing objectives directly pertinent to operational efficiency and safety needs for multimodal travelers at a signalized intersection.

RESEARCH OBJECTIVES

The problem aforementioned is rooted in the inherent difficulty of incorporating an instantaneously changeable S_p into the current PCI timing procedure. It is believed that automated pedestrian detectors provide significant operational and safety benefits when installed in conjunction with pedestrian pushbuttons at actuated traffic signals (*16*). Previous studies have evaluated a spectrum of potential pedestrian-detection technologies including microwave (*16, 17*), active- or passive-infrared (*16–18*), video imaging, ultrasonic, and piezoelectric sensors. In Europe, PUFFIN (pedestrian user friendly intelligent) uses microwave and passive-infrared sensors to detect presence or absence of pedestrians on midblock crosswalks (*19*). This research hypothesizes that similar sensors effectively capture pedestrians to meet data-input needs in intersection control, and then the PCI duration can be dynamic to reflect the crossing time in instantaneous needs, mitigating the intersectionwide vehicle flow inefficiency. Inspired by the methodological transition toward the artificial intelligence domain, this research developed a traffic signal system prototype that not only realizes a dynamic accommodation for crossing pedestrians but also incorporates FLC into fulfilling multifaceted motorized vehicle needs. This research also quantified the potential benefits from the new system, which was optimized by genetic algorithm (GA), in comparison with a standard signal system in prevalent application.

INTELLIGENT SIGNAL SYSTEM

Applications of fuzzy sets and fuzzy logic to traffic signal controls originated in the 1970s. The first known attempt was made by Pappis and Mamdani (*20*), who conducted a simulation study of a fuzzy logic controller at a one-way signalized intersection. Chang and Shyu produced a fuzzy expert system to evaluate whether a signal is required for an intersection (*21*). Kim studied the fuzzy algorithms of isolated intersections and discussed the turning traffic problem (*22*). Niittymaki and Kikuchi developed a fuzzy logic controller for a pedestrian crosswalk, and the controller provided a pedestrian friendly control while keeping vehicle delays smaller than conventional controls (*23*). Trabia et al. presented a fuzzy logic–based adaptive signal controller for an intersection with conflicting movements (*24*). The controller produced fewer vehicle delays than the traffic-actuated controller. Murat and Gedizlioglu developed an FLC-based signal model for isolated intersections and compared it with the traffic-actuated simulation and other specific vehicle-actuated models (*25*). They found that the fuzzy model operationally outperformed previous models. Lu and Noyce (*26*) and Lu et al. (*27*) developed fuzzy systems to signalize midblock crosswalks and roundabouts. Simulation experiments revealed that the FLC-based signal controls outperform a common system in manifold aspects. However, no research work has ever integrated a dynamic nonmotorized traveler control holistically into an FLC-based intersection signal system to improve multimodal safety and operations; that omission motivated this engineering endeavor.

Phasing Scheme

To signalize an intersection means to continuously determine the reasonable time point for switching the right-of-way between conflicting movements. In principle, traffic signal control is a decision-making process of determining, at time intervals, whether to extend or terminate the current vehicle green, while guaranteeing safe pedestrian accommodation. The FLC implements a complex decision-making process for determining green termination time. From systems engineering perspectives, if the logic structure in the phasing scheme is overly sophisticated, perhaps its interaction with the FLC process can result in more intractable variables and then pose potential impairments to the efficiency in systematic optimization. In this philosophy, a sensible balance should be maintained between the phasing simplification and the decision-making complexity. Figure 2*a* depicts a four-phase scheme that offers the flexibility of skipping left-turn (LT) phases if LT traffic demands are absent. Usually right-turn-on-red is permitted for intersection signalization in North America. Green starts with either (*a*) an exclusive LT phase (Φ1 or Φ3) followed by a through (TH) phase (Φ2 or Φ4) or (*b*) a TH phase (Φ2 or Φ4) followed by an LT phase (Φ3 or Φ1) or a TH phase (Φ4 or Φ2).

Operational States

The vehicle green control for most traffic signal systems is universal in temporal structure—minimum and maximum greens delimit a time range during which the control logic plays a role in making an extension or termination decision by identifying the emergence of specific operational states. At time steps (Δt), the FLC-based signal system recognizes a specific operational state at a specific time point ($T + \Delta t$) to navigate its logic flow. On the basis of Figure 2*a*, all operational states are defined by certain time step–based variables for vehicle greens and constant parameters for signal timing limits, as follows:

- The Φ2 (or Φ4) min-over state occurs if $t_{\Phi 2}^G(T + \Delta t) \geq G_{\Phi 2}^{min}$ {or $t_{\Phi 4}^G(T + \Delta t) \geq G_{\Phi 4}^{min}$},
- The Φ2 (or Φ4) max-out state occurs if $t_{\Phi 2}^G(T + \Delta t) \geq G_{\Phi 2}^{max}$ {or $t_{\Phi 4}^G(T + \Delta t) \geq G_{\Phi 4}^{max}$},
- The Φ1 (or Φ3) green-over state occurs if $t_{\Phi 1}^G(T + \Delta t) \geq G_{\Phi 1}$ {or $t_{\Phi 3}^G(T + \Delta t) \geq G_{\Phi 3}$}, and
- The Φ2 (or Φ4) PCI max-out state occurs if $t_{\Phi 2}^G(T + \Delta t) \geq W_{\Phi 2} + PCI_{\Phi 2}^{max}$ {or $t_{\Phi 4}^G(T + \Delta t) \geq W_{\Phi 4} + PCI_{\Phi 4}^{max}$}

where

$t_{\Phi 2}^G(T + \Delta t)$, $t_{\Phi 4}^G(T + \Delta t)$ = green length already displayed for Φ2, Φ4 at $(T + \Delta t)$;
$G_{\Phi 2}^{min}$, $G_{\Phi 4}^{min}$ = minimum timing limits for Φ2, Φ4 vehicle green display;
$G_{\Phi 2}^{max}$, $G_{\Phi 4}^{max}$ = maximum timing limits for Φ2, Φ4 vehicle green display;
$W_{\Phi 2}$, $W_{\Phi 4}$ = walk interval length in parallel with Φ2, Φ4 ($W_{\Phi 2} < G_{\Phi 2}^{min}$, $W_{\Phi 4} < G_{\Phi 4}^{min}$);
$t_{\Phi 1}^G(T + \Delta t)$, $t_{\Phi 3}^G(T + \Delta t)$ = vehicle green length already displayed for Φ1, Φ3 at $(T + \Delta t)$;
$G_{\Phi 1}$, $G_{\Phi 3}$ = vehicle green length preset for Φ1, Φ3; and
$PCI_{\Phi 2}^{max}$, $PCI_{\Phi 4}^{max}$ = maximum timing limit for the PCI interval in parallel with Φ2, Φ4; $G_{\Phi 2}^{max} < PCI_{\Phi 2}^{max} + W_{\Phi 2}$, $G_{\Phi 4}^{max} < PCI_{\Phi 4}^{max} + W_{\Phi 4}$.

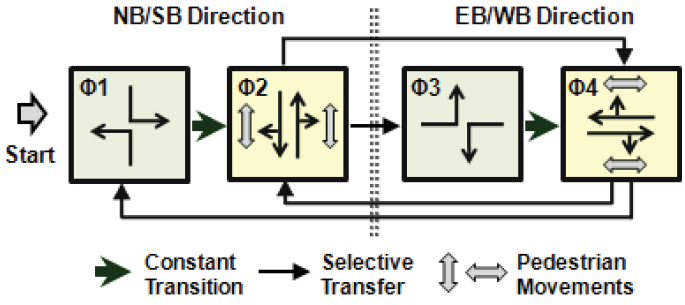

(a)

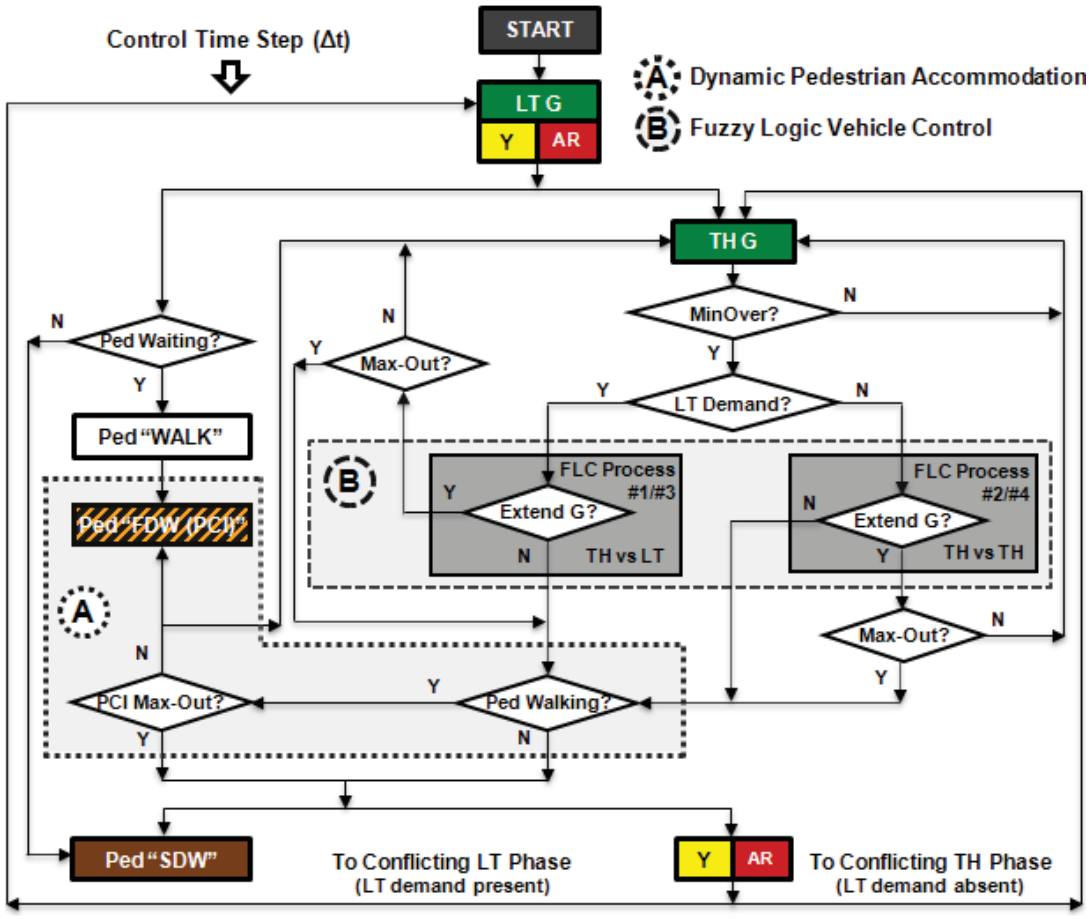

(b)

FIGURE 2 Two intersection traffic signal systems under study: (*a*) phasing scheme diagram of FLC signal system and (*b*) control logic flowchart of FLC signal system (NB = northbound; SB = southbound; EB = eastbound; WB = westbound).

(continued on next page)

FLC Variables

The system has four FLC processes: Process 1 (Φ2 versus Φ3), Process 2 (Φ2 versus Φ4), Process 3 (Φ4 versus Φ1), and Process 4 (Φ4 versus Φ2) (Figure 2*b*). The time step (Δt) incrementally proceeds, and one process operates to evaluate ongoing operations through fuzzifying the input variables below for inference engine and defuzzifier, which make the decision, with output variables, concerning the control action on current vehicle green in Φ2 or Φ4.

Input Variables

Traffic Intensity Level The traffic intensity level (vehicles/lane) that prevails on TH lanes of the current phase (Φ2, Φ4) in the last time step (Δt).

$$x^c_{\Phi 2}(T+\Delta t) \text{ and } x^c_{\Phi 4}(T+\Delta t)$$

The variables denote the average number of vehicles between paired detectors for TH lanes, reflecting the magnitude of traffic

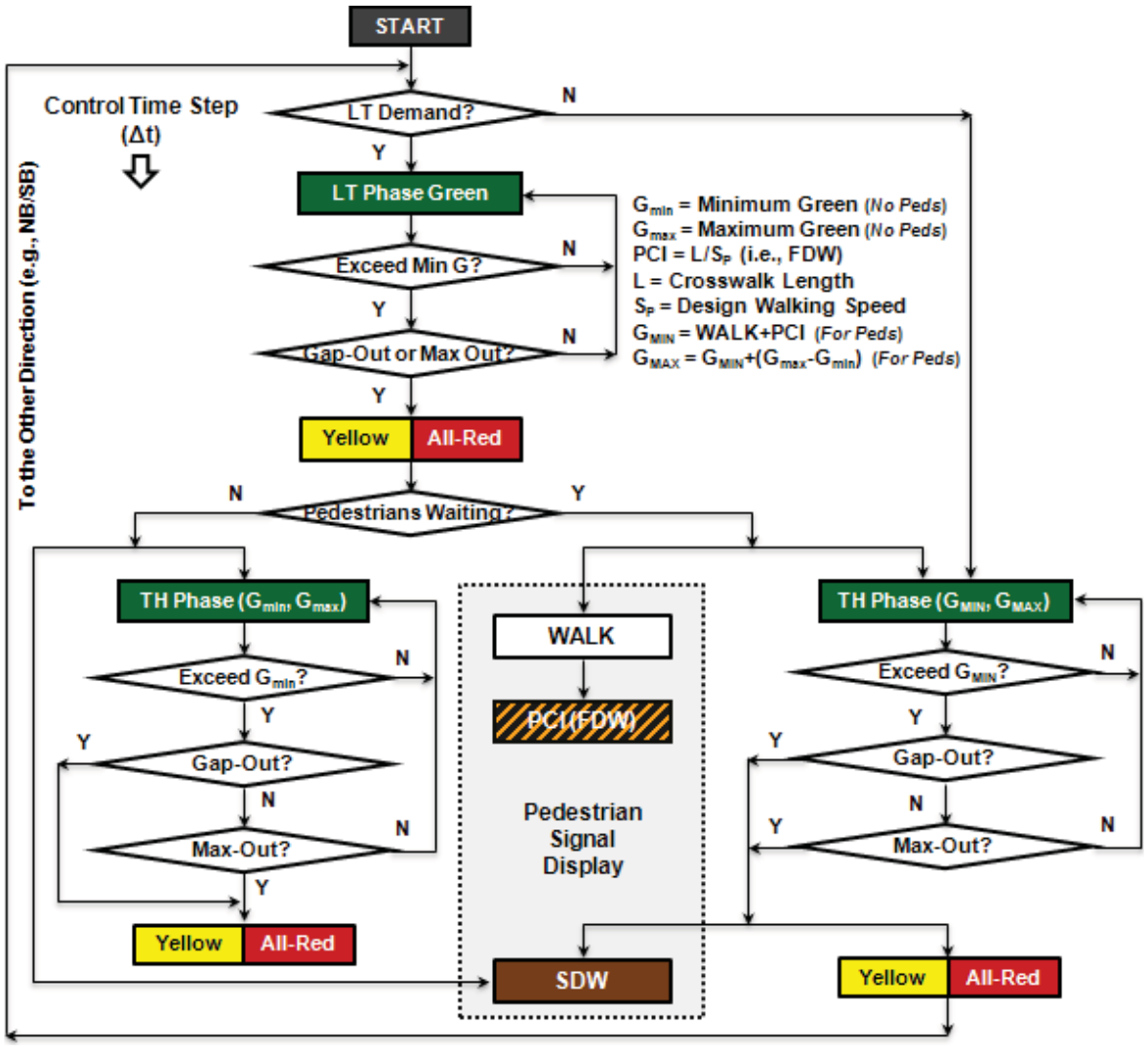

(c)

FIGURE 2 *(continued)* Two intersection traffic signal systems under study: (*c*) control logic flowchart of standard dual-ring, eight-phase, vehicle-actuated controller (NEMA) system (Y = yes; N = no).

demand to be met. These variables address the issue of operational efficiency in dissipating vehicles at an intersection. It should be reasonable to assume that the more intensely vehicle flows prevail, the more desirously they demand the green display. Each variable has sparse, moderate, and intense fuzzy sets.

Vehicle Discharge Headway The vehicle discharge headway (seconds/lane) that appears on TH lanes of the current phase (Φ2, Φ4) in the last time step (Δt).

$$y^c_{\Phi 2}(T+\Delta t) \text{ and } y^c_{\Phi 4}(T+\Delta t)$$

The variables, which represent the time gap between two adjacent vehicles traversing across the stop line, embody a safety-related factor in dissipating vehicles. The larger value for opposite approaches was captured. It is believed that the smaller the headway is, the more probably vehicles are packed; the larger the headway is, the more probably a platoon is proceeding (*23*). Each variable has short and long fuzzy sets.

Average Queue Length The average queue length (vehicles/lane) that accumulates for the next phase (Φ3, Φ4; Φ1, Φ2) in the last time step (Δt).

$$z^n_{\Phi 3}(T+\Delta t) \text{ and } z^n_{\Phi 4}(T+\Delta t); z^n_{\Phi 1}(T+\Delta t) \text{ and } z^n_{\Phi 2}(T+\Delta t)$$

The variables, which quantify how many vehicles have been queuing in TH lanes or LT bays, encompass an operational and safety-related element in serving vehicles. It should be inferable that the longer a vehicle has been waiting for green lights, the more inclined the driver is to commit signal incompliance as a result of aggravating impatience. Each variable has so-so, tolerable, and frustrating fuzzy sets.

Output Variables

$w_{\Phi 2}(T+\Delta t)$ and $w_{\Phi 4}(T+\Delta t)$ represent the control action taken by the FLC process on Φ2, Φ4 at the time point $(T+\Delta t)$: termination and extension.

Control Logic

Figure 2*b* demonstrates how the control logic operates—at time steps, one FLC process always determines extension or termination.

Constant Φ1 → Φ2 Transition

Start with Φ1. At the time point $(T + \Delta t)$ at which the Φ1 green-over state occurs, Φ2 starts.

Selective Φ2 Control Process

If pedestrians exist, Walk starts, to last until $W_{\Phi 2}$ is reached. Simultaneously, $G_{\Phi 2}^{\min}$ is satisfied to dissipate queuing vehicles. At the time point $(T + \Delta t)$ at which the Φ2 min-over state occurs, the system activates one FLC process by examining whether Case A or Case B is true.

Case A. Present F3 Demand In this case, the system activates Process 1, which operates on the basis of $x_{\Phi 2}^{c}(T + \Delta t)$, $y_{\Phi 2}^{c}(T + \Delta t)$, and $z_{\Phi 3}^{n}(T + \Delta t)$. At the end of Δt, Process 1 takes action on the current green via $w_{\Phi 2}(T + \Delta t)$:

1. If the current green extends, the parallel PCI persists concurrently. When green extensions continue until the Φ2 max-out state occurs, the vehicle detection–based FLC process stops and the system determines whether Condition I or Condition II is true.
2. If the current green ends, the system determines whether Condition I or Condition II is true.

Case B. Absent F3 Demand In this case, the system activates Process 2, which operates on the basis of $x_{\Phi 2}^{c}(T + \Delta t)$, $y_{\Phi 2}^{c}(T + \Delta t)$, and $z_{\Phi 4}^{n}(T + \Delta t)$. At the end of Δt, Process 2 takes the action on the current green:

1. If the current green extends, the parallel PCI continues equally. When the Φ2 max-out state occurs, the fuzzy process stops and the system identifies the trueness in Condition I or Condition II.
2. If the current green terminates, the system identifies Condition I or Condition II.

Condition I. Vacant Crosswalks If pedestrian sensors discover that all pedestrians have vacated intersection crosswalks, $w_{\Phi 2}(T + \Delta t)$ takes termination and the next appropriate phase is activated: for Case A, Φ3 starts; for Case B, Φ4 starts.

Condition II. Occupied Crosswalks If pedestrian sensors recognize that pedestrians still occupy crosswalks, the PCI and the parallel vehicle green persist together. Hence, slower pedestrians are fully protected by the PCI display. When all pedestrians disappear from crosswalks, the system terminates Φ2 to activate the next phase: for Case A, Φ3 starts; for Case B, Φ4 starts. When these PCI extensions continue until the Φ2 PCI max-out state occurs, Φ2 unconditionally ceases and the next appropriate phase starts.

To consummate a signal cycle, the logic in Φ2 will be iterated in Φ4, after the Φ3 to Φ4 transition (if applicable) finishes. In summary, the input variables are involved in an FLC process as follows:

Process 1:

$$x_{\Phi 2}^{c}(T + \Delta t),\ y_{\Phi 2}^{c}(T + \Delta t),\ z_{\Phi 3}^{n}(T + \Delta t)$$

Process 2:

$$x_{\Phi 2}^{c}(T + \Delta t),\ y_{\Phi 2}^{c}(T + \Delta t),\ z_{\Phi 4}^{n}(T + \Delta t)$$

Process 3:

$$x_{\Phi 4}^{c}(T + \Delta t),\ y_{\Phi 4}^{c}(T + \Delta t),\ z_{\Phi 1}^{n}(T + \Delta t)$$

Process 4:

$$x_{\Phi 4}^{c}(T + \Delta t),\ y_{\Phi 4}^{c}(T + \Delta t),\ z_{\Phi 2}^{n}(T + \Delta t)$$

FLC Configuration

The fuzzifier uses specific membership functions to transform these input variables into fuzzy values processable for the inference engine. Trapezoid membership function was used to simplify the problem, which is mathematically defined by $\max\{\min[(x-s)/(t-s), 1, (n-x)/(n-m)], 0]\}$ and the breakpoints (m, n, s, t) (*2*). Figures 3*a* to 3*c* show these membership functions and basic parameters (h_n, i_n, j_n, k_n; u_n, v_n; w_n, x_n, y_n, z_n).

Resembling an intelligent brain, the inference engine contains "if . . . and . . . then . . ." rules that linguistically describe operational conditions in current and next phases. Tables 1 and 2 show the generic format of a rule base. The statements after "if" and "then" are called "premise" and "consequence," respectively. "And" is called "operator," and all operators interconnect premises to establish a rule base. The inference engine reaches a conclusion by identifying the similarity between an input (a, b, c) and some premises $(A_1, B_1, C_1; \ldots; A_i, B_i, C_i; \ldots; A_N, B_N, C_N)$. An input can trigger multiple rules because the input and the premises in triggered rules are represented by fuzzy sets and fuzzy relationships. Hence, all consequences from different rules are strictly valid, and then they are aggregated for an output space consisting of fuzzy control actions. To be defuzzified for a final decision, the output space is a compromise between these conclusions from all triggered rules. Essentially, all inference rules are indirectly intertwined with pursuing operational and safety goals for intersection users: (*a*) pedestrians are accommodated safely and timely; (*b*) vehicles are served timely to avoid signal noncompliances, and a platoon is dissipated entirely to prevent rear-end collisions (*23*). Table 2 exhibits the rule base for FLC Process 1. Synoptically, this system was designed to manage the intersection to satisfy safety and operational needs for multimodal travelers. FLC can be flexible, robust, and adaptive in tackling dynamic intersection operations because membership functions implicitly span a vast range of possibilities. The Mamdani and Assilian method was used for the aggregation process, which was based on Zadeh's work on fuzzy algorithms for complex systems and decision processes (*28, 29*). This method was among the first control systems built by using fuzzy set theory, which was proposed as an effort to control a steam engine and boiler by synthesizing linguistic rules from experienced human operators.

A defuzzifier transforms the output space into a final decision. Several techniques have been developed to reach a final crisp output. Traditional methods include maximum criterion, mean of maximum,

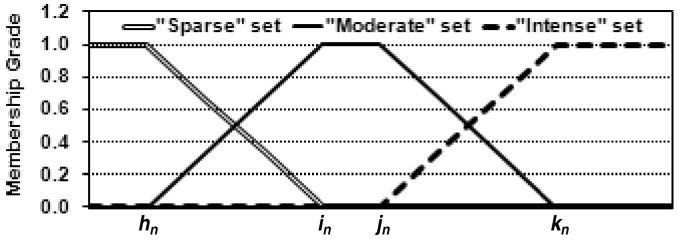

(a)

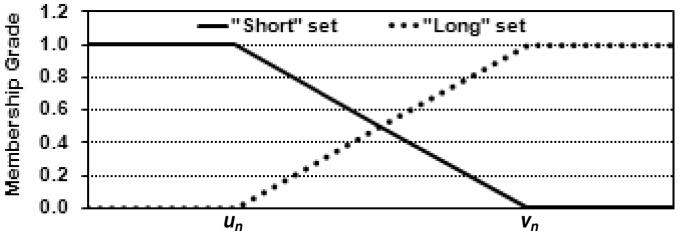

(b)

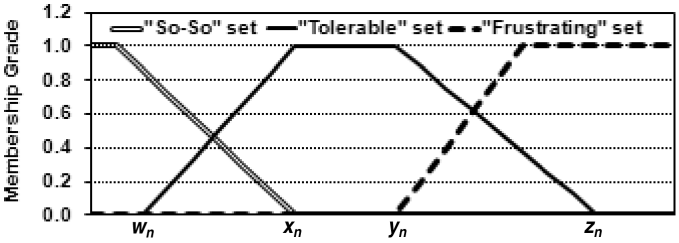

(c)

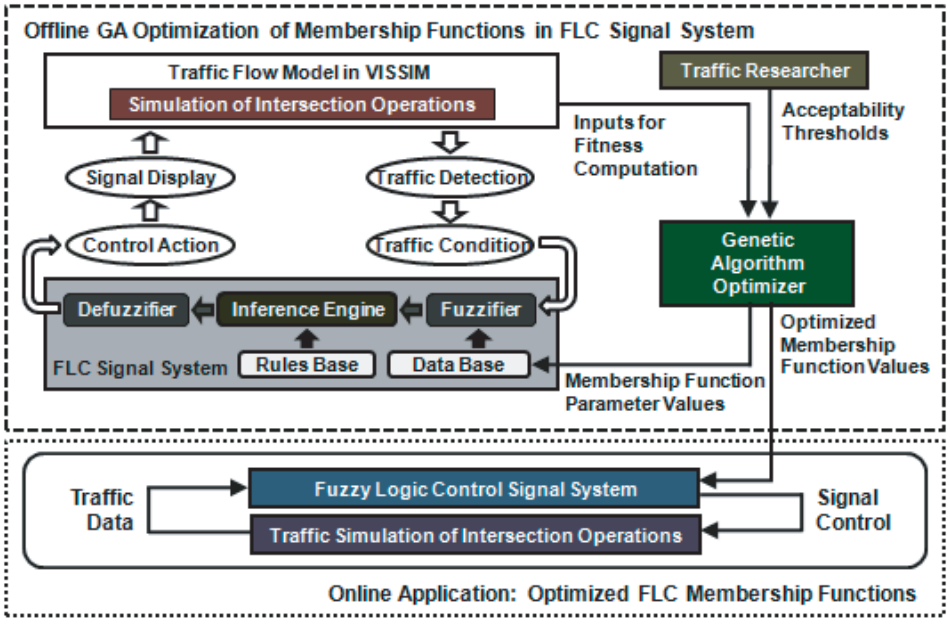

(d)

FIGURE 3 FLC signal system optimization: (*a*) traffic intensity level membership function, (*b*) discharge headway membership function, (*c*) queue length membership function, and (*d*) GA-based optimization framework.

TABLE 1 Fuzzy Logic Inference Engine for Intersection FLC Signal System—Section A: Generic Format of Fuzzy Logic Rules

Fuzzy Rule	Premise (Crisp Inputs: $X = a$, $Y = b$, $Z = c$)	Consequence
Rule 1	IF {x is "A_1"} AND {y is "B_1"} AND {z is "C_1"}	THEN {"E[a]" or "T[b]"}
Rule i	IF {x is "A_i"} AND {y is "B_i"} AND {z is "C_i"}	THEN {"E" or "T"}
Rule N	IF {x is "A_N"} AND {y is "B_N"} AND {z is "C_N"}	THEN {"E" or "T"}
Crisp output	{"E" or "T"}	
Where	x, y, z = input (state) variables related to traffic conditions, a, b, c = values of input variables, and A_i, B_i, C_i = natural language expressions (fuzzy sets) for traffic conditions, $i = 1, \ldots, N$.	

[a]Terminate current vehicle green.
[b]Extend current vehicle green.

and center of gravity, each of which is effective for distinct problems (*30*). The maximum criterion method is the reasonable choice because of the binary characteristic in traffic signal control (*26, 27*).

GA Optimization

The methods for establishing inference engine and defuzzifier are normative in FLC applications, whereas those for formulating databases supported by membership functions are mostly subjective and prone to engender biases. GA proves powerful in resolving combinatorial optimization problems (*31*). Here a GA optimizer was developed in C++ to tune all parameters of membership functions in FLC processes. Figure 3*d* depicts the systematic optimization framework.

Algorithmic Logic

GA is underpinned by the principle of evolution and survival of the fittest; the terminology is borrowed from natural genetics (*32*). The optimization procedure iterates by generations. In each generation, the procedure maintains a population of chromosomes, each of which links genes in linear succession. Each chromosome resembles a candidate solution. Initially, the procedure starts with a randomly generated population. Each solution is evaluated quantitatively for its fitness for survival. Then, a new population is formed by selecting more fit solutions; some solutions undergo alterations through crossover and mutation operators to yield new solutions. The process of evaluation, selection, and alteration iterates for generations and heuristically converges to a near-optimum solution (*33*).

TABLE 2 Fuzzy Logic Inference Engine for Intersection FLC Signal System—Section B: Inference Rule Base in FLC Process 1 (Φ2 versus Φ3)

Discharge Headway $\{y^c_{\Phi 2}(T+\Delta t)\}$	Approach Flow Level $\{x^c_{\Phi 2}(T+\Delta t)\}$		
	Sparse	Moderate	Intense
Short			
Queue length $\{z^n_{\Phi 3}(T+\Delta t)\}$			
So-so	T	E	E
Tolerable	T	T	E
Frustrating	T	T	T
Long			
Queue length $\{z^n_{\Phi 3}(T+\Delta t)\}$			
So-so	T	E	E
Tolerable	T	T	E
Frustrating	T	T	T

Implementation Design

GA needs a genetic solution representation, an initial population, a fitness evaluation function, a more fit selection procedure, genetic operators that alter the composition of solutions, and control parameters concerning the population size and the probabilities of adopting genetic operators.

Representation Scheme A generic scheme was used to transform a solution into a binary string. Each individual parameter bounded between minimum and maximum values is treated as a gene whose binary string was fixed at a length of 6 in. In this case, an encoding procedure transformed the decimal values of parameters into integers that are represented by binary strings, as Equation 3 shows (*34*). To convert the binary strings back to their decimal values, the decoding schema was used as shown in Equation 4:

$$X_i = \frac{X_i^{\min} + d_i\left(X_i^{\max} - X_i^{\min}\right)}{\left(2^L - 1\right)} \tag{3}$$

$$d_i = \frac{\left[\left(2^L - 1\right)\left(X_i - X_i^{\min}\right)\right]}{\left(X_i^{\max} - X_i^{\min}\right)} \tag{4}$$

where

X_i = transformed value of the ith parameter, $i = 1, 2, \ldots, 40$;
$X_i^{\min}$ = minimum value as the lower bound for the ith parameter;
$X_i^{\max}$ = maximum value as the upper bound for the ith parameter;
L = length of the binary string for a candidate solution (i.e., chromosome); and
d_i = decimal value of the parameter.

Initial Population The initial population size was set to 30 solutions, each of which included 40 parameters. The initial values of all

parameters were randomly determined within their corresponding reasonable bounds.

Evaluation and Selection The solution evaluation included running the new signal system with 40 parameters encoded into a binary string and determining the fitness value in regard to the inverse of overall measure-of-effectiveness defined as the weighted average of classical performance measures: $\alpha \cdot$ (average pedestrian delay) + $\beta \cdot$ (average total delay per vehicle) + $\gamma \cdot$ (average number of stops per vehicle); $\alpha + \beta + \gamma = 1.00$, $\alpha = \beta = 0.30$. The roulette wheel procedure selected the more fit solutions from each population. The probability of being selected was directly proportionate to the fitness values, and then two solutions were randomly chosen by using these probabilities to create new solutions in the next generation.

Genetic Operators The mutation operator randomly selected a gene and replaced it with a random number selected between that gene's bounds. Such genes were within their new permissible ranges. If any gene was not, a new random number (selected from the new bounds) replaced it. One digit of each parameter was randomly chosen, and one was mutated to zero and zero to one. The crossover operator combined the features of two parent solutions to form two new solutions by switching corresponding segments of parents.

Control Parameters Identifying appropriate values for control parameters is more an art than a science (*33*). These values were determined after initial experiments: population size = 30; crossover probability = .60; mutation probability = .05. In total, 60 generations were run because of demanding computational requirements.

SYSTEM EVALUATION

Practical limitations make it almost infeasible to conduct an easy evaluation in real-world contexts, so an in-lab platform should be used as a surrogate approach in which the FLC system can be implemented precisely and evaluated quantifiably. Today, traffic simulation is essential in transportation research given its cost-effectiveness, unobtrusiveness, risk-free nature, and high-speed feature. VISSIM, a microsimulation tool, is applied worldwide because of its powerful traveler-modeling capability, infallible multimodal detectability, unrestrained signal-control-logic flexibility by vehicle-actuated programming, convenient data processability per input or output files, and seamless application interface via object-oriented programming tools (*35*).

Comparison Strategy

In the VISSIM environment, the FLC system was compared with the standard dual-ring, eight-phase, vehicle-actuated controller extensively deployed and conventionally cited as NEMA (National Electrical Manufacturers Association) control (*5*). Approximately 15% of the pedestrian population walks more slowly, at a speed less than 3.5 ft/s (*36*). Therefore, the mean walking speed was conservatively set to 3.0 ft/s. To reflect previous findings, a researcher-customized speed distribution was modeled with maximum and minimum walking speeds set to 8.0 ft/s and 1.0 ft/s. The dynamic PCI function provides full signal protection for all modeled pedestrians, some of whom walk at the lowest speed (S_p = 1.0 ft/s). Then, to maintain a uniform degree of signal protection in one comparison case, the static PCI in the vehicle-actuated controller (NEMA) was timed, adopting S_p = 1.0 ft/s to guarantee equivalently adequate PCI duration—this adoption follows the philosophy to which the aforementioned countermeasure resorts. Furthermore, the *Manual on Uniform Traffic Control Devices* PCI timing standard in current practice makes it necessary to investigate another case that uses S_p = 3.5 ft/s (*15*). For both NEMA-based comparison cases, G_{min} rises to G_{MIN} = PCI + Walk when pedestrians are present and the in-between period ($G_{max} - G_{min}$) is maintained to determine new maximum green (G_{MAX}) (Figure 2*c*).

Test Intersection

This research used FHWA's next generation simulation project data and summary report for an urban intersection under NEMA control (*37*). This intersection has four typical multilane approaches that receive TH, RT (right-turn), and LT vehicular movements. A pedestrian crosswalk lies downstream from each of the four stop lines. Figure 4 shows the test intersection and these virtually deployed detectors.

Study Scenarios

Two vehicle flow levels of mixed traffic composition were examined: existing flows and high-demands conditions. The observed traffic volumes at the test intersection established the existing flows condition, and the proportion of trucks and buses in observed traffic composition is very low (*37*). To explore additional scenarios, all observed volumes were augmented at a fixed rate (40%) to create the high-demands condition, which approaches the maximum capacity. Two pedestrian flow levels were investigated: moderate, which equals 50 pedestrians per hour per two-way crosswalk (pphpc), and crowded, which equals 150 pphpc. Hence, four operational situations were modeled and combined with three comparison cases to yield 12 study scenarios. The analysis period spanned is 1 h.

Timing Settings

As Tables 3 and 4 show, most signal timing data in the next generation simulation project were used for the NEMA control in existing flows condition. For the high-demands condition, NEMA green timings for the existing flows condition were proportionally enhanced to meet enlarged traffic demands. For the FLC system, TH green timings maintain a consistence with NEMA's counterparts; the FLC system's LT greens take values higher than the averages for NEMA's LT greens.

Performance Measures

HCM prescribes level-of-service criteria for multimodal travelers at signalized intersections by using average control delay and average pedestrian delay (*11*). Traffic simulation is increasingly used as a standard method to address operational issues that cannot be effectively addressed by HCM-based or other analytical procedures (*38*). VISSIM tracks individual traveler interactions to compute individual delays and measures average total delay as the difference in travel time at a lower speed compared with that at the free-flow speed (*35*).

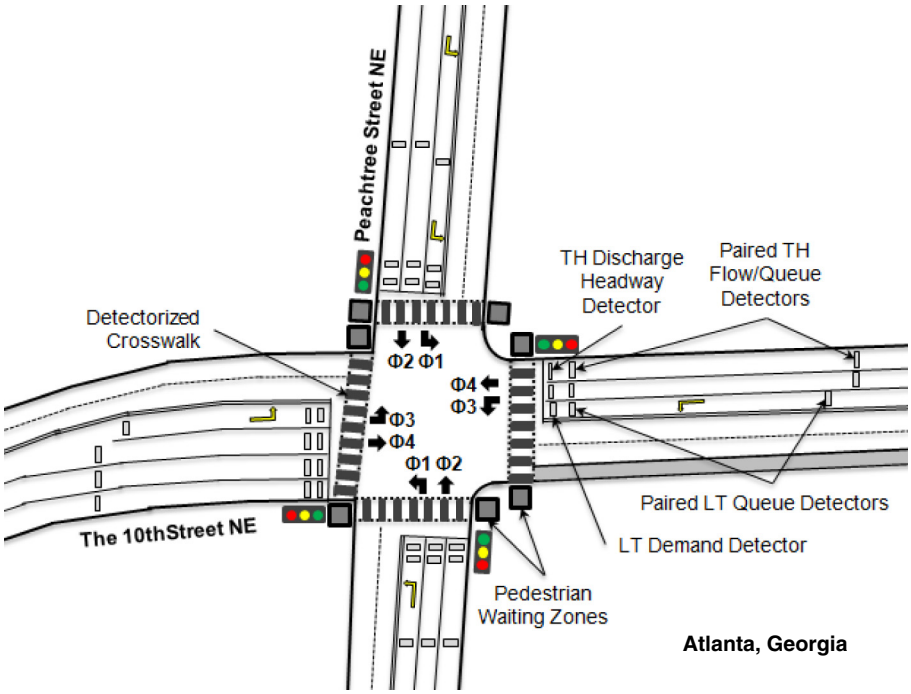

FIGURE 4 Test intersection and placement of approach detectors for FLC signal system (NE = northeast).

TABLE 3 Basic Signal Timing Settings for Three Comparison Cases: Standard Dual-Ring, Eight-Phase, Vehicle-Actuated Controller (NEMA Traffic Signal System)

Basic Signal Timings (s) [Static FDW (PCI)]	Existing Flows Traffic Condition								High-Demands Traffic Condition							
	LT Phase				TH (and RT) Phase				LT Phase				TH (and RT) Phase			
	I	III	V	VII	II	IV	VI	VIII	I	III	V	VII	II	IV	VI	VIII
Green interval (no pedestrians)																
G_{min}	5.0	8.0	8.0	5.0	15.0	12.0	15.0	16.0	6.0	10.0	10.0	6.0	19.0	15.0	19.0	20.0
G_{max}	10.0	15.0	10.0	15.0	45.0	30.0	45.0	30.0	13.0	19.0	13.0	19.0	57.0	38.0	57.0	38.0
Green interval (with pedestrians)																
G_{MIN}[a]	5.0	8.0	8.0	5.0	61.0	74.0	61.0	74.0	6.0	10.0	10.0	6.0	61.0	74.0	61.0	74.0
G_{MAX}[a]	10.0	15.0	10.0	15.0	91.0	92.0	91.0	88.0	13.0	19.0	13.0	19.0	99.0	97.0	99.0	92.0
G_{MIN}[b]	5.0	8.0	8.0	5.0	23.0	26.0	23.0	26.0	6.0	10.0	10.0	6.0	23.0	26.0	23.0	26.0
G_{MAX}[b]	10.0	15.0	10.0	15.0	53.0	44.0	53.0	40.0	13.0	19.0	13.0	19.0	61.0	49.0	61.0	44.0
Intergreen interval																
Yellow	4.0	4.0	4.0	4.0	4.0	4.0	4.0	4.0	4.0	4.0	4.0	4.0	4.0	4.0	4.0	4.0
All-red	1.0	1.0	1.0	1.0	1.0	1.0	1.0	1.0	1.0	1.0	1.0	1.0	1.0	1.0	1.0	1.0
Pedestrian interval																
Walk	—	—	—	—	7.0	7.0	7.0	7.0	—	—	—	—	7.0	7.0	7.0	7.0
PCI[a]	—	—	—	—	54.0	67.0	54.0	67.0	—	—	—	—	54.0	67.0	54.0	67.0
PCI[b]	—	—	—	—	16.0	19.0	16.0	19.0	—	—	—	—	16.0	19.0	16.0	19.0

NOTE: NEMA System: Phases I and VI–WB (westbound), Phases III and VIII–NB (northbound), Phases II and V–EB (eastbound), Phases IV and VII–SB (southbound). G_{max} and G_{MAX} = maximum greens, G_{min} and G_{MIN} = minimum greens, G_{MIN} = Walk + PCI, $G_{MAX} = G_{MIN} + (G_{max} - G_{min})$, PCI = L/S_p. — = not applicable.
[a]When design walking speed S_p = 1.0 ft/s for the PCI (FDW) timing.
[b]When design walking speed S_p = 3.5 ft/s for the PCI (FDW) timing.

TABLE 4 Basic Signal Timing Settings for Three Comparison Cases: FLC-Based Traffic Signal System

Basic Signal Timings (s) [Dynamic FDW (PCI)]	Existing Flows Traffic Condition				High-Demands Traffic Condition			
	LT Phase		TH (and RT) Phase		LT Phase		TH (and RT) Phase	
	Φ1	Φ3	Φ2	Φ4	Φ1	Φ3	Φ2	Φ4
Green interval								
G_{LT}	13.0	10.0	—	—	16.0	13.0	—	—
min G_{TH}	—	—	12.0	15.0	—	—	15.0	19.0
max G_{TH}	—	—	30.0	45.0	—	—	38.0	57.0
Intergreen interval								
Yellow	4.0	4.0	4.0	4.0	4.0	4.0	4.0	4.0
All-red	1.0	1.0	1.0	1.0	1.0	1.0	1.0	1.0
Pedestrian interval								
Walk	—	—	7.0	7.0	—	—	7.0	7.0

NOTE: FLC system: Φ1 and Φ2 (NB–SB), Φ3 and Φ4 (EB–WB), $G_{LT} - G_{\Phi 1}$ and $G_{\Phi 3}$, min $G_{TH} = G_{\Phi 2}^{min}$ and $G_{\Phi 4}^{min}$, max $G_{TH} = G_{\Phi 2}^{max}$ and $G_{\Phi 4}^{max}$.

Therefore, total delay includes HCM-related control delay and delays from other conditions (*39*). Ideally, the goals of minimizing total delay can maximize the intersection capacity utilization and reduce the potential for accident-producing conflicts. By definition, a vehicle is queued if its speed drops below 5.0 km/h and remains under 10 km/h (*35*). VISSIM reports average and maximum queues observed during the analysis period by using the current queue length measured upstream every time step. Number of stops denotes the total number of all occasions in which a vehicle enters the queue condition (*35*). Average number of vehicle stops is believed to be related to the frequency of occurrence of rear-end collisions besides the association with delays. VISSIM reports average stops per vehicle in the 1-h period.

Simulation Data

Commonly, transportation studies evaluate intersection performance by averaging multiple simulation results for varied operational situations (*40*). Here, six replications, with unique random seeds on disparate magnitude levels, were conducted for NEMA-related study scenarios to accommodate the stochastic variations from underlying random models. Each replication lasted 3,600 simulation seconds. During run time, an external program, as an automation client in seamless dialogue with the VISSIM-based server, periodically captured, aggregated, computed, and exported the simulation data. With all random seeds used as a pool, the GA optimizer contains a module that randomizes the assignment of random seeds to individual runs for the sake of statistical correlation and computational efficiency.

RESEARCH RESULTS

Results for moderate and crowded pedestrians in existing flows and high-demand conditions of comparison cases are shown in Figure 5 and Figure 6, respectively. NEMA results are reported with arithmetic means of six replications. Table 5 shows the optimized membership function parameters. The performance measures for a motorized vehicle denote the weighted averages on the basis of cars, trucks, and buses involved in a study scenario; measures for a user unit account for all motorized vehicles and pedestrians.

Existing Flows Condition

As shown in Figure 5*a,* with moderate pedestrian flows the NEMA 1.0-ft/s case generates much higher average total delay for each travel mode than does the FLC system. For instance, the FLC system tremendously reduces the average total delay per user unit by 61.17%, from 89.46 s to 34.74 s; per motorized vehicle by 62.20%, from 88.80 s to 33.57 s; and per pedestrian by 52.12%, from 96.27 s to 46.09 s. Simultaneously, average total delays generated in the NEMA 3.5-ft/s case are close to those in the FLC system. For example, average total delays are 32.49 s and 34.74 s per user unit, 30.95 s and 33.57 s per motorized vehicle, and 47.77 s and 46.09 s per pedestrian for the 3.5-ft/s case and the FLC system, respectively. Figure 5*a* also demonstrates that in contrast to the NEMA 1.0-ft/s case, the FLC system sharply decreases the average number of stops for vehicles. For example, it diminishes the average stops per motorized vehicle (or car) from 1.04 to 0.74 by 28.85%, per truck from 1.05 to 0.60 by 42.86%, and per bus from 1.03 to 0.79 by 23.30%. In addition, the average number of stops generated in the NEMA 3.5-ft/s case closely approximates the counterparts in the FLC case. For example, the average number of stops is 0.71 s and 0.74 s per motorized vehicle (or car) for the 3.5-ft/s case and the FLC case, respectively.

Figure 5*b* shows, with crowded pedestrians, that the performance measures are universally enhanced from their counterparts in Figure 5*a* and unveils the operational impact of pedestrian flows. For instance, average total delay per car produced in the NEMA 3.5-ft/s case varies from 30.87 s to 33.92 s, and average stops per bus generated in the FLC case ascends from 0.79 to 1.18. Figure 5*b* shows that the FLC system significantly lessens average total delay per user unit from 98.14 s to 44.00 s, per car from 98.72 s to 39.11 s, per truck from 99.10 s to 41.63 s, per bus from 88.07 s to 49.86 s, and per pedestrian from 96.60 s to 59.36 s. The FLC case also largely decreases average number of stops per motorized vehicle (or car) from 1.17 to 0.77, per truck from 1.19 to 0.85. Similar to results shown in Figure 5*a,* the performance

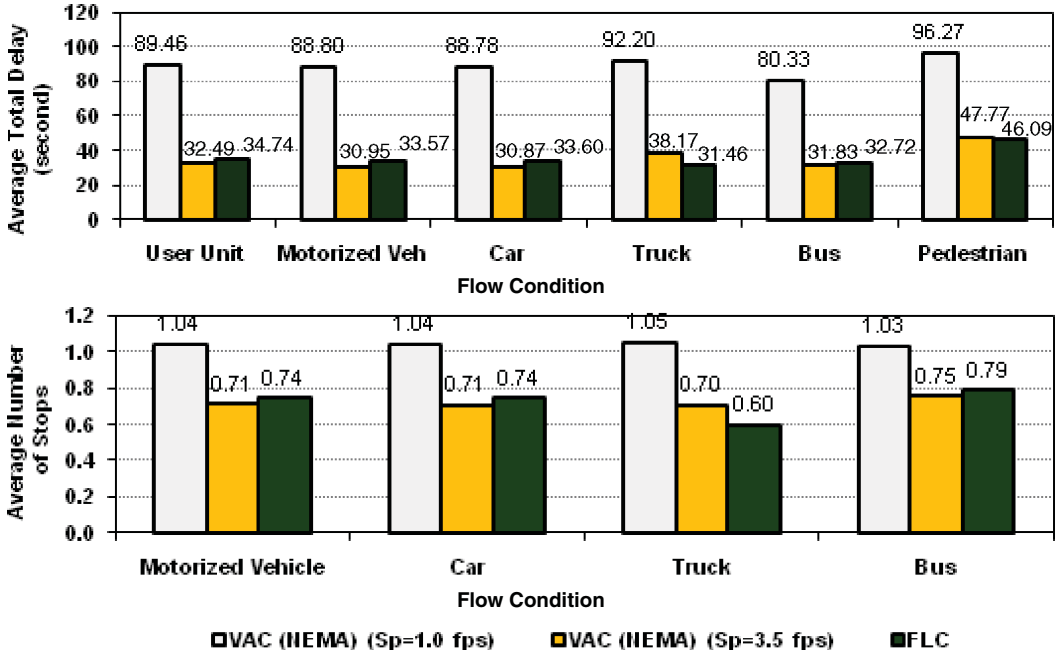

(a)

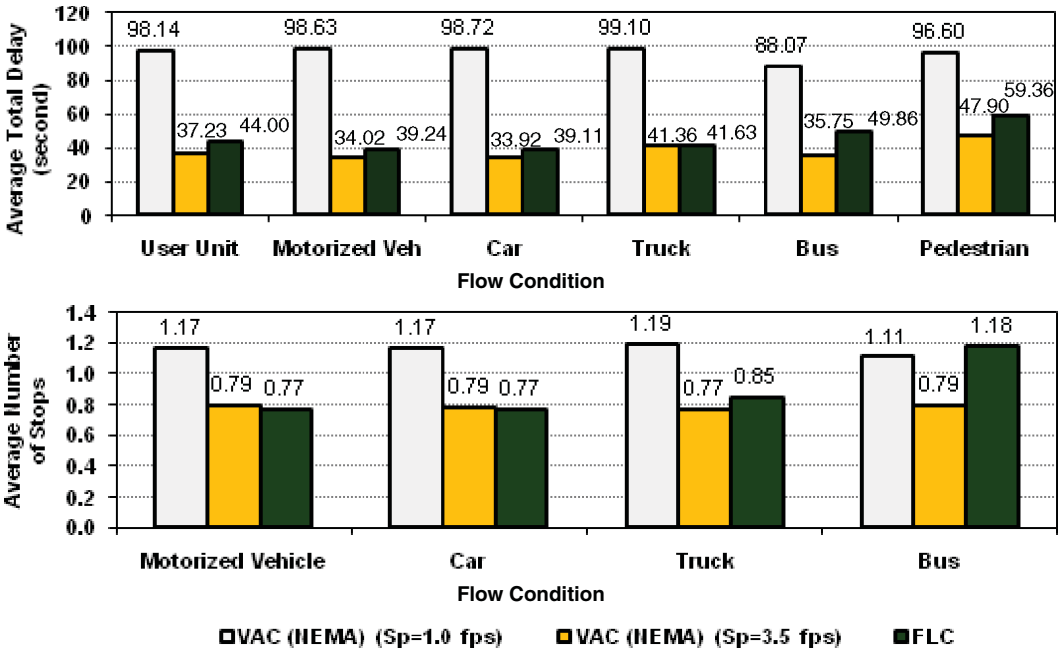

(b)

FIGURE 5 Average total delay and number of stops under existing flows condition: (*a*) moderate (50 pphpc) pedestrian flow level and (*b*) crowded (150 pphpc) pedestrian flow level.

measures in the NEMA 3.5-ft/s case are fairly close to those in the FLC case.

High-Demands Condition

Figure 6*a* shows that, compared with the NEMA 1.0-ft/s case, the FLC system substantially lowers average total delay per user unit from 157.35 s to 43.56 s, per motorized vehicle from 161.71 s to 42.90 s, and per pedestrian from 105.02 s to 52.04 s. For user unit and pedestrian, the average total delay generated in the NEMA 3.5-ft/s case is not much different from that in the FLC case; respectively, average total delays are 36.06 s and 43.56 s per user unit, 35.01 s and 42.90 s per motorized vehicle, 50.68 s and 52.04 s per pedestrian for the 3.5-ft/s case and the FLC system. Figure 6*a* shows that the FLC case enormously decreases the average number of

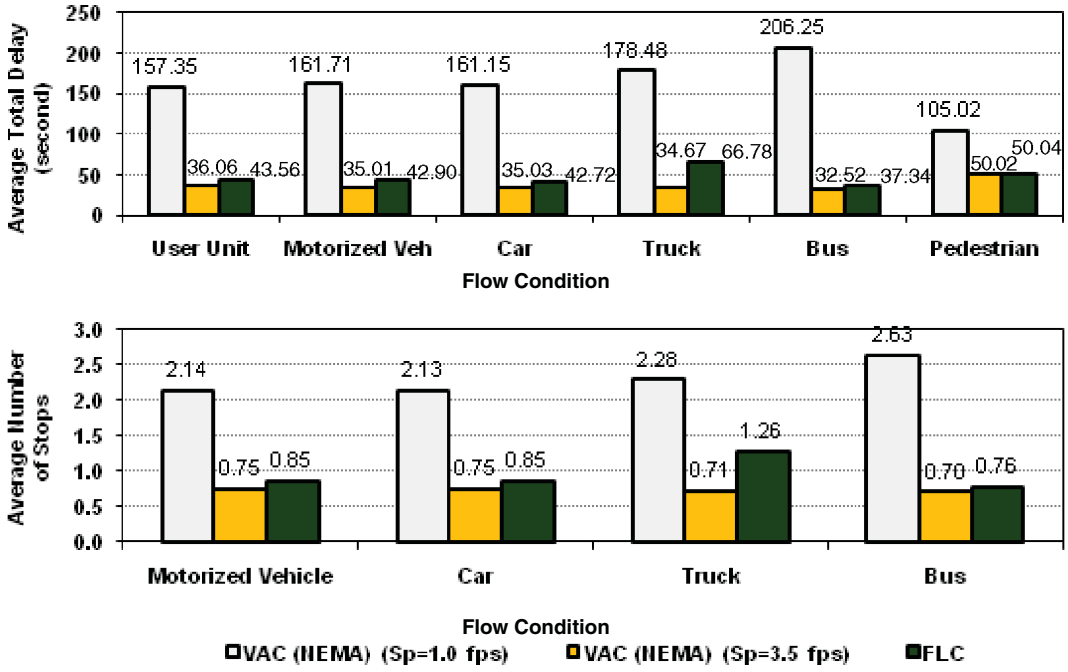

(a)

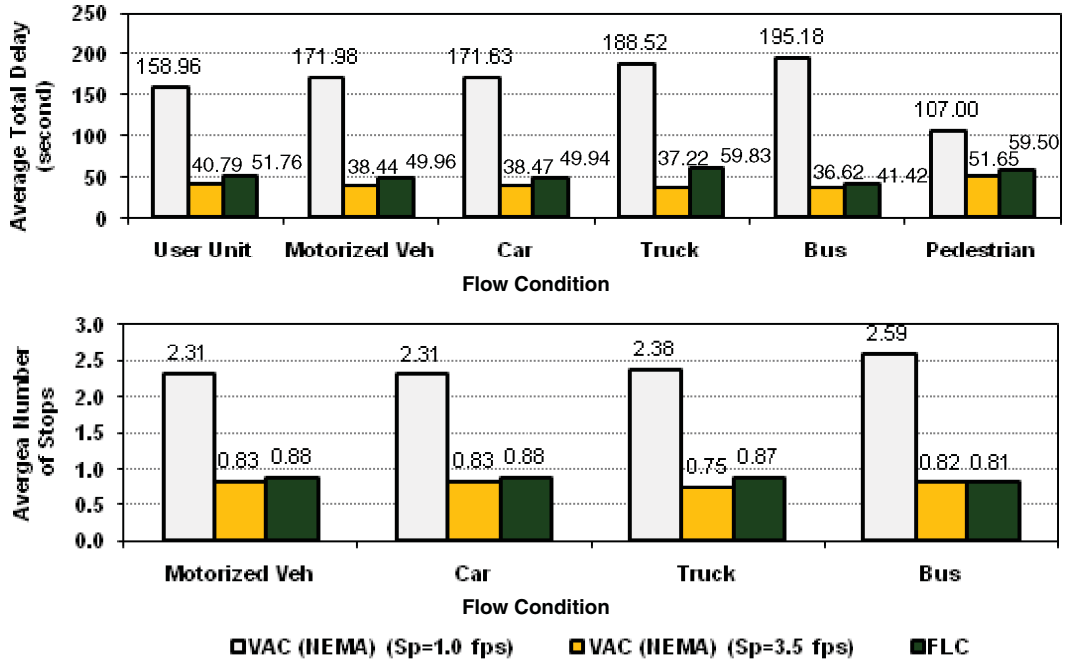

(b)

FIGURE 6 Average total delay and number of stops under high-demands condition: (*a*) moderate (50 pphpc) pedestrian flow level and (*b*) crowded (150 pphpc) pedestrian flow level (VAC = vehicle-actuated controller).

stops per motorized vehicle from 2.14 to 0.85, per car from 2.13 to 0.85, per truck from 2.28 to 1.26, per bus from 2.63 to 0.76. For each motorized vehicle (or car), the average number of stops created in the NEMA 3.5-ft/s case roughly approximates that in the FLC case, which is 0.75 s and 0.85 s, respectively.

As shown in Figure 6*b*, with a crowded pedestrian flow level, most performance measures for each mode are enlarged compared with their counterparts under moderate flow levels, as shown in Figure 6*a*. For instance, average total delay per car in the NEMA 1.0-ft/s case changes from 161.15 s to 171.63 s, and average number of stops per bus by the FLC system rises from 0.76 to 0.81. Compared with the 1.0-ft/s case, the FLC system considerably lessens average total delay per user unit from 158.96 s to 51.76 s, per motorized vehicle from 171.98 s to 49.96 s, per pedestrian from

TABLE 5 Optimized Parameters for Membership Functions in FLC Processes

Optimized Membership Function Parameter	Trapezoid Membership Function for Each Input Variable									
	Traffic Intensity Level				Discharge Headway		Average Queue Length			
	h_n	i_n	j_n	k_n	u_n	v_n	w_n	x_n	y_n	z_n
FLC Process: Existing Flows Vehicles and Moderate Pedestrians										
1	1.83	5.61	7.12	8.02	0.88	2.40	2.25	2.79	3.75	4.71
2	0.79	5.74	6.98	8.02	0.63	1.48	2.81	3.98	4.45	5.50
3	3.26	5.99	6.07	7.55	1.96	2.28	2.31	2.47	3.87	4.52
4	2.50	5.36	6.79	7.12	0.79	1.17	1.24	3.31	3.55	5.69
FLC Process: Existing Flows Vehicles and Crowded Pedestrians										
1	3.36	4.28	7.07	7.12	1.74	2.02	1.42	2.90	3.15	4.08
2	3.45	6.31	7.31	7.83	0.88	1.80	1.24	2.83	3.60	6.26
3	1.40	3.90	4.50	7.79	1.45	1.77	1.77	2.83	3.23	4.59
4	2.12	5.17	5.55	6.12	2.40	2.47	2.95	5.02	5.40	6.79
FLC Process: High-Demands Vehicles and Moderate Pedestrians										
1	1.21	4.79	6.50	7.17	2.02	2.40	2.40	2.47	3.63	4.52
2	1.07	5.29	6.26	6.31	1.96	1.99	2.29	3.88	5.88	5.93
3	2.60	4.28	4.79	6.83	2.31	2.44	1.71	2.63	4.34	4.37
4	1.21	4.02	6.36	7.31	0.75	2.28	3.48	3.79	6.26	6.31
FLC Process: High-Demands Vehicles and Crowded Pedestrians										
1	0.98	5.74	6.83	8.07	1.80	2.40	0.63	2.31	3.27	5.00
2	2.12	4.91	7.12	7.64	1.36	2.31	3.24	4.50	5.60	7.26
3	2.26	4.47	6.60	7.36	0.94	1.07	1.33	2.07	2.60	3.06
4	1.45	5.36	6.17	7.45	1.71	2.44	2.62	4.02	4.93	7.17

NOTE: n = 1, 2, 3, and 4 for FLC Processes 1, 2, 3, and 4, respectively.

107.00 s to 59.50 s. The differences between average total delays in the NEMA 3.5-ft/s case and the FLC case are not relatively considerable: 40.79 s and 51.76 s per user unit, 51.65 s and 59.50 s per pedestrian, respectively, for the 3.5-ft/s case and the FLC system. The FLC system substantially alters the average number of stops per motorized vehicle (or car) from 2.31 to 0.88, in comparison with the 1.0-ft/s case. The difference between average number of stops for the 3.5-ft/s case and the FLC system are very small for motorized vehicles and cars (0.83 versus 0.88).

CONCLUDING REMARKS

An FLC-based traffic signal system was developed for a typical urban intersection where pedestrians prevail. During each signal phase, the dynamic PCI offers pedestrians crossing time in real-time needs; operational efficiency, safety, and human factors were incorporated into the vehicle green control process. On simulation platform, the performance of the novel system optimized by GA was evaluated against the standard dual-ring, eight-phase, vehicle-actuated control (NEMA) system, which adopted different design walking speeds.

The results in NEMA's 1.0-ft/s case indicate that although all pedestrians are protected by adequate PCI duration, the intersection operations have been in breakdown. Therefore, the current countermeasure, which simplistically lowers the design walking speed, was operationally deficient. The results in NEMA's 3.5-ft/s case are close to or a little lower than those for the FLC system. However, the 3.5 ft/s standard cannot offer crossing protection for pedestrians walking more slowly than that speed. Furthermore, the NEMA control omits multifaceted vehicle needs in decision-making logic, which governs the green by rigid unit-extension rule and never thinks about ongoing intersectionwide situations in current and next phases to better safety and operations. In contrast, the FLC system provides full pedestrian protection via dynamic PCI and also fulfills manifold vehicle needs (e.g., safer platoon dissipation, shorter queue) with competitive performance, which realizes a reasonable compromise between competing objectives in intersection control.

The new system relinquishes a fixed walking speed as a timing input, closing the debate on the most appropriate design pedestrian. This research first addressed the issue of how to integrate all intersection users holistically into a systematic improvement framework by means of an innovative signal system that dynamically accommodates pedestrians and intelligently serves vehicles. The application of this system to a transportation network is beneficial particularly to urban contexts in which numerous multimodal travelers traverse daily. With more than 272,000 traffic signals nationwide (*41*), the potential impact of the intellectual merit here could be significant from perspectives of multimodal safety, operational efficiency, and quality of life for the traveling public.

FUTURE RESEARCH

Hardware-in-the-loop simulation can more realistically evaluate the performance of the system transplanted onto a physical controller (*42, 43*). A key issue in ultimate applications is accuracy and reliability of pedestrian sensors, so a sufficient number of field experiments are necessary to appraise how the deployable system performs in efficacy, reliability, and sensitivity. The offline optimized parameters can work in relation to traffic-responsive plan selection; using time-of-day schedules or observed multimodal operational situations, the system triggers appropriate timing plans configured with a set of optimized parameters to procure the intended benefits under varied scenarios. It is certainly worthwhile to advance the optimization in online direction (*6*). Merely focused on isolated intersections in free operations, this research inspires the further exploration of how the system plays a part in coordinated arterials. It is very meaningful to integrate the system optimization synthetically with microscopic emissions modeling (*44*) and surrogate safety assessment methodology (*45*).

ACKNOWLEDGMENTS

The authors thank Teresa Adams, Bin Ran, and Jessica Guo of the Department of Civil and Environmental Engineering and Yu-Hen Hu of the Department of Electrical and Computer Engineering at the University of Wisconsin–Madison for their sound advice. Peter Rafferty of the Traffic Operations and Safety Laboratory of the University of Wisconsin–Madison is much appreciated for his kind remarks. The authors also express their sincere thanks to the anonymous reviewers, who offered constructive comments.

REFERENCES

1. Kikuchi, S. Artificial Intelligence in Transportation Analysis: Approaches, Methods, and Applications. In *Transportation Research Part C,* Vol. 17, No. 5, 2009, p. 455.
2. Kosko, B. *Fuzzy Logic.* Art House, Helsinki, Finland, 1993.
3. Kikuchi, S. Application of Fuzzy Set Theory to the Analysis of Transportation Problems. Presented at 2nd International Conference on Applications of Advanced Technologies in Transportation Engineering. Minneapolis, Minn., 1991.
4. Meyer, M. *A Toolbox for Alleviating Traffic Congestion and Enhancing Mobility.* ITE, Washington, D.C., 1997.
5. Roess, P., E. Prassas, and W. McShane. *Traffic Engineering,* 3rd ed. Pearson Prentice Hall, Upper Saddle River, N.J., 2004.
6. Liu, H. X., J.-S. Oh, and W. Recker. Adaptive Signal Control System with Online Performance Measure for a Single Intersection. In *Transportation Research Record: Journal of the Transportation Research Board, No. 1811,* Transportation Research Board of the National Academies, Washington, D.C., 2002, pp. 131–138.
7. Dubois, D., and H. Prade. *Fuzzy Sets and Systems: Theory and Applications.* Academic Press, New York, 1980.
8. NHTSA. *Traffic Safety Facts 2008: Pedestrians.* http://www-nrd.nhtsa.dot.gov/Pubs/811163.pdf. Accessed May 16, 2010.
9. Insurance Institute for Highway Safety (IIHS). *Fatality Facts 2008, Pedestrians.* http://www.iihs.org/research/fatality_facts_2008/pedestrians.html. Accessed May 16, 2010.
10. *USA Today* (online news). Cities Try to Improve Crosswalk Safety. www.usatoday.com/news/nation/2008-02-24-crosswalk_N.htm. Accessed March 1, 2008.
11. *Highway Capacity Manual.* TRB, National Research Council, Washington, D.C., 2000.
12. Fitzpatrick, K., M. A. Brewer, and S. M. Turner. Another Look at Pedestrian Walking Speed. In *Transportation Research Record: Journal of the Transportation Research Board, No. 1982,* Transportation Research Board of the National Academies, Washington, D.C., 2006, pp. 21–29.
13. Gates, T. J., D. A. Noyce, A. R. Bill, and N. Van Ee. Recommended Walking Speeds for Timing of Pedestrian Clearance Intervals Based on Characteristics of the Pedestrian Population. In *Transportation Research Record: Journal of the Transportation Research Board, No. 1982,* Transportation Research Board of the National Academies, Washington, D.C., 2006, pp. 38–47.
14. Arango, J., and J. Montufar. Walking Speed of Older Pedestrians Who Use Canes or Walkers for Mobility. In *Transportation Research Record: Journal of the Transportation Research Board, No. 2073,* Transportation Research Board of the National Academies, Washington, D.C., 2008, pp. 79–85.
15. *Manual on Uniform Traffic Control Devices (MUTCD),* 2009 ed. FHWA, U.S. Department of Transportation, 2009.
16. Hughes, R., H. Huang, C. Zegeer, and M. Cynecki. Automated Detection of Pedestrians in Conjunction with Standard Pedestrian Push Buttons at Signalized Intersections. In *Transportation Research Record: Journal of the Transportation Research Board, No. 1705,* TRB, National Research Council, Washington, D.C., 2000, pp. 32–39.
17. Beckwith, D. M., and K. M. Hunter-Zaworski. Passive Pedestrian Detection at Unsignalized Crossings. In *Transportation Research Record 1636,* TRB, National Research Council, Washington, D.C., 1998, pp. 96–103.
18. Noyce, D., A. Gajendran, and R. Dharmaraju. Development of Bicycle and Pedestrian Detection and Classification Algorithm for Active-Infrared Overhead Vehicle Imaging Sensors. In *Transportation Research Record: Journal of the Transportation Research Board, No. 1982,* Transportation Research Board of the National Academies, Washington, D.C., 2006, pp. 202–209.
19. Davies, H. E. H. *The PUFFIN Pedestrian Crossing: Experience with the First Experimental Sites.* Research Report 364. Transport Research Laboratory, Berkshire, United Kingdom, 1992.
20. Pappis, C., and E. Mamdani. A Fuzzy Logic Controller for a Traffic Junction. In *IEEE Transactions on Systems, Man, and Cybernetics,* Vol. SMC-7, No. 10, 1977, pp. 707–717.
21. Chang, Y.-H., and T.-H. Shyu. Traffic Signal Installation by the Expert System Using Fuzzy Set Theory for Inexact Reasoning. *Transportation Planning and Technology,* Vol. 17, No. 2, 1993, pp. 191–202.
22. Kim S. *Applications of Petri Networks and Fuzzy Logic to Advanced Traffic Management Systems.* PhD dissertation. Polytechnic University, New York, 1994.
23. Niittymaki, J., and S. Kikuchi. Application of Fuzzy Logic to the Control of a Pedestrian Crossing Signal. In *Transportation Research Record 1651,* TRB, National Research Council, Washington, D.C., 1998, pp. 30–38.
24. Trabia, M., M. Kaseko, and M. Ande. A Two-Stage Fuzzy Logic Controller for Traffic Signals. *Transportation Research Part C,* Vol. 7, No. 6, 1999, pp. 353–367.
25. Murat, Y., and E. Gedizlioglu. A Fuzzy Logic Multi-Phased Signal Control Model for Isolated Junctions. *Transportation Research Part C,* Vol. 13, No. 1, 2005, pp. 19–36.
26. Lu, G., and D. A. Noyce. Pedestrian Crosswalks at Midblock Locations: Fuzzy Logic Solution for Existing Signal Operations. In *Transportation Research Record: Journal of the Transportation Research Board, No. 2140,* Transportation Research Board of the National Academies, Washington, D.C., 2009, pp. 63–78.
27. Lu, G., F. Guan, and D. A. Noyce. Multimodal Accessibility of Modern Roundabouts: Intelligent Management System Versus Common Signalization Scheme. In *Transportation Research Record: Journal of the Transportation Research Board, No. 2183,* Transportation Research Board of the National Academies, Washington, D.C., 2010, pp. 103–119.
28. Mamdani, E., and S. Assilian. An Experiment in Linguistic Synthesis with a Fuzzy Controller. *International Journal of Man–Machine Studies,* Vol. 7, No. 1, 1975, pp. 1–13.
29. Zadeh, L. Outline of a New Approach to the Analysis of Complex Systems and Decision Processes. *IEEE Transactions on Systems, Man, and Cybernetics,* Vol. SMC-3, No. 1, 1973, pp. 28–44.
30. Yager, R., and D. Filev. *Essentials of Fuzzy Modeling and Control.* John Wiley & Sons, New York, 1994, p. 384.
31. Park, B., C. J. Messer, and T. Urbanik II. Enhanced Genetic Algorithm for Signal-Timing Optimization of Oversaturated Intersections. In *Transportation Research Record: Journal of the Transportation Research Board, No. 1727,* TRB, National Research Council, Washington, D.C., 2000, pp. 32–41.
32. Sadek, A. W., B. L. Smith, and M. J. Demetsky. Dynamic Traffic Assignment: Genetic Algorithms Approach. In *Transportation Research Record 1588,* TRB, National Research Council, Washington, D.C., 1997, pp. 95–103.

33. Michalewicz, Z. *Genetic Algorithms + Data Structures = Evolutionary Programs.* Springer-Verlag, Berlin, 1994.
34. Arslan, A., and M. Kaya. Determination of Fuzzy Logic Membership Functions Using Genetic Algorithms. In *Fuzzy Sets and Systems,* Vol. 118, No. 2, 2001, pp. 297–306.
35. *VISSIM 5.10 User Manual.* Planung Transport Verkehr (PTV) AG, Karlsruhe, Germany, 2008.
36. Kell, J., and I. Fullerton. *Manual of Traffic Signal Design.* ITE, Washington, D.C., 1982.
37. Cambridge Systematics, Inc. *NGSIM Peachtree Street (Atlanta) Data Analysis.* Summary Report for FHWA, June 2007.
38. Elefteriadou, L., J. D. Leonard II, G. List, H. Lieu, M. Thomas, R. Giguere, G. Johnson, and R. Brewish. Beyond the *Highway Capacity Manual:* Framework for Selecting Simulation Models in Traffic Operational Analyses. In *Transportation Research Record: Journal of the Transportation Research Board, No. 1678,* TRB, National Research Council, Washington, D.C., 1999, pp. 96–106.
39. Tian, Z. Z., T. Urbanik II, R. Engelbrecht, and K. Balke. Variations in Capacity and Delay Estimates from Microscopic Traffic Simulation Models. In *Transportation Research Record: Journal of the Transportation Research Board, No. 1802,* Transportation Research Board of the National Academies, Washington, D.C., 2002, pp. 23–31.
40. Abdy, Z. R., and B. R. Hellinga. Use of Microsimulation to Model Day-to-Day Variability of Intersection Performance. In *Transportation Research Record: Journal of the Transportation Board, No. 2088,* Transportation Research Board of the National Academies, Washington, D.C., 2008, pp. 18–25.
41. ITE. Traffic Signals 101 Press Release. *National Traffic Signal Report Card.* 2007. http://www.ite.org/reportcard/signals101.asp. Accessed Feb. 13, 2011.
42. Ghaman, R., L. Zhang, G. Mchale, and C. Stallard. The Role of Traffic Simulation in Traffic Signal Control System Development. *Proc., 2003 IEEE International Conference on Intelligent Transportation Systems,* Vol. 1, Shanghai, China, IEEE, Piscataway, N.J., 2003, pp. 872–877.
43. Bullock, D., B. Johnson, R. Wells, M. Kyte, and Z. Li. Hardware-in-the-Loop Simulation. *Transportation Research Part C,* Vol. 12, No. 1, 2004, pp. 73–89.
44. Stevanovic, A., J. Stevanovic, K. Zhang, and S. Batterman. Optimizing Traffic Control to Reduce Fuel Consumption and Vehicular Emissions: Integrated Approach with VISSIM, CMEM, and VISGAOST. In *Transportation Research Record: Journal of the Transportation Research Board, No. 2128,* Transportation Research Board of the National Academies, Washington, D.C., 2009, pp. 105–113.
45. Gettman, D., and L. Head. Surrogate Safety Measures from Traffic Simulation Models. In *Transportation Research Record: Journal of the Transportation Board, No. 1840,* Transportation Research Board of the National Academies, Washington, D.C., 2003, pp. 104–115.

The Traffic Signal Systems Committee peer-reviewed this paper.